

## The influence of the anolyte solution type and concentration on lithium migration in mortar specimens

Souza, L. M.S.; Polder, R. B.; Çopuroğlu, O.

**DOI**

[10.1016/j.conbuildmat.2018.07.073](https://doi.org/10.1016/j.conbuildmat.2018.07.073)

**Publication date**

2018

**Document Version**

Final published version

**Published in**

Construction and Building Materials

**Citation (APA)**

Souza, L. M. S., Polder, R. B., & Çopuroğlu, O. (2018). The influence of the anolyte solution type and concentration on lithium migration in mortar specimens. *Construction and Building Materials*, 186, 123-130. <https://doi.org/10.1016/j.conbuildmat.2018.07.073>

**Important note**

To cite this publication, please use the final published version (if applicable). Please check the document version above.

**Copyright**

Other than for strictly personal use, it is not permitted to download, forward or distribute the text or part of it, without the consent of the author(s) and/or copyright holder(s), unless the work is under an open content license such as Creative Commons.

**Takedown policy**

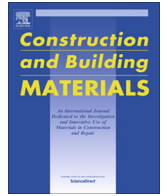
Please contact us and provide details if you believe this document breaches copyrights. We will remove access to the work immediately and investigate your claim.

***Green Open Access added to TU Delft Institutional Repository***

***'You share, we take care!' - Taverne project***

**<https://www.openaccess.nl/en/you-share-we-take-care>**

Otherwise as indicated in the copyright section: the publisher is the copyright holder of this work and the author uses the Dutch legislation to make this work public.



# The influence of the anolyte solution type and concentration on lithium migration in mortar specimens

L.M.S. Souza<sup>a,\*</sup>, R.B. Polder<sup>a,b</sup>, O. Çopuroğlu<sup>a</sup>

<sup>a</sup> Delft University of Technology, Delft, The Netherlands

<sup>b</sup> TNO Technical Sciences/Structural Reliability, Delft, The Netherlands

## HIGHLIGHTS

- A study on the influence of the anolyte solution on lithium migration is presented.
- Results indicate that anolyte concentration, rather than type, affected migration.
- Anolytes with highest concentrations led to highest levels of lithium in specimens.

## ARTICLE INFO

### Article history:

Received 18 September 2017

Received in revised form 19 June 2018

Accepted 11 July 2018

Available online 21 July 2018

### Keywords:

Alkali-silica reaction (ASR)

Migration

Lithium

Anolyte solution

## ABSTRACT

Electrochemical lithium migration has been suggested as repair technique for alkali-silica reaction affected concrete structure. In this method, an electric field is used to transport lithium into the material. Current studies have used anolyte solutions with various lithium salts at different concentrations. However, little has been said on the effect of the anolyte on lithium migration. In this paper, an experimental study on the influence of the type of lithium compound and its concentration in the anolyte is presented. Results point out that the concentration of the solution, rather than the type of lithium salt, affected migration. The anolytes with the highest concentrations provided the highest final levels of lithium in the specimens.

© 2018 Elsevier Ltd. All rights reserved.

## 1. Introduction

Even though alkali-silica reaction (ASR) affects many concrete structures worldwide, currently, there are limited repair options available [1,2]. In this framework, electrochemical lithium migration has been suggested as an intervention method.

The use of lithium-based admixtures to suppress ASR expansion has been known for decades (e.g. [3–5]). It has been proposed that lithium ions alter the reaction mechanism either by hindering the reaction or by altering the product into a less-expansive one [1,6–8]. In existing concrete structures, however, lithium ions can no longer be incorporated into the fresh mixture. In this case, the ions need to be transported into the material and electrochemical lithium migration has shown to be the most effective technique to do so [9,10].

Driving lithium ions into concrete by means of an electrical field was first suggested by Page [11]. He theorized that, if a lithium

solution was used as anolyte during an electrochemical chloride extraction treatment of a structure, lithium ions would migrate towards the reinforcing steel and mitigate the effects of ASR. Since then, a number of studies have been published (e.g. [9,10,12–19]), with divergent conclusions.

In current literature, several different lithium salts have been used in the anolyte solution, at different concentrations, under voltages up to 60 V. Nevertheless, little has been discussed on the reason behind the choice of those solutions or on whether the choice would influence the final results. In fact, Ueda [20] investigated the effect of different lithium compounds. However, the concentration of the anolyte solutions was not discussed. In this article, the influence of different lithium solutions on migration will be addressed.  $\text{Li}_2\text{CO}_3$ ,  $\text{LiOH}$  and  $\text{LiNO}_3$  were the lithium salts chosen to be tested at concentrations varying from 0.2 to 7.8 M.  $\text{LiOH}$  and  $\text{LiNO}_3$  were considered because of their high solubility in water. Although  $\text{Li}_2\text{CO}_3$  has very low solubility in water, Ueda [14] noted in his work that  $\text{Li}_2\text{CO}_3$  solution leads to higher effective diffusion coefficient than  $\text{LiOH}$  (when tested in a two-chamber set-up).

\* Corresponding author at: Pontifical Catholic University of Rio de Janeiro, Rua Marquês de São Vicente, 225, Ed. Cardeal Leme, r. 315, Brazil.

E-mail address: [imsilvadesouza@esp.puc-rio.br](mailto:imsilvadesouza@esp.puc-rio.br) (L.M.S. Souza).

## 2. Experimental program

### 2.1. Materials and specimen preparation

Mortar specimens were prepared with water to cement ratio (w/c) of 0.5 and sand to cement proportion of 3:1. The mixing procedure followed the standard NEN-EN 196-1 [21]. The air void content was measured as 1.0% (NEN-EN 12350-7 [22]) and the flow value, obtained by the flow table test (NEN-EN 12350-5 [23]), was 270 mm.

Ordinary Portland cement type CEM I 42.5 N, commercially available in the Netherlands (ENCI), was used. Its chemical composition is shown in Table 1. In addition, CEN standard sand with  $D_{max}$  of 2 mm (according to EN 196 1:2005) and deionized water were used. Cylindrical specimens, with diameter of 98 mm and height of 50 mm, were cast and cured in a fog room ( $20.0 \pm 2.0^\circ\text{C}$  and R.H. of  $96 \pm 2\%$ ) for 36 days before the beginning of the experiment.

### 2.2. Methods

Lithium migration testing was performed in the set-up described by ASTM 1202 [24]. As shown in the scheme of Fig. 1(a), a specimen was placed between two acrylic chambers filled with solution, each with a stainless steel mesh as electrode. Each chamber contained 270 ml of electrolyte solution. Once the electric potential was applied between the electrodes, cations were attracted by the cathode (negative electrode), whereas anions moved in the opposite direction, towards the anode (positive electrode). Fig. 1(b) shows one of the experimental cells. The experiments were carried out in a climate controlled laboratory, at  $20.0 \pm 2.0^\circ\text{C}$  and R.H. of  $50 \pm 5\%$ .

Saturated  $\text{Ca}(\text{OH})_2$  solution (0.02 M) was used as catholyte in all tests. The anolytes, on the other hand, were solutions of different lithium compounds, at different concentrations, as shown in Table 2. The highest concentration of each lithium compound solution is its saturation (or near saturation) concentration. Lithium compounds with higher solubility were also tested in lower concentrations, as the table shows. It is worth noting that  $\text{Li}_2\text{CO}_3$  0.2 M solutions had lithium concentration of 0.4 M while the other 0.2 M solutions had 0.2 M of lithium. The range of anolyte concentrations was chosen so that the solutions would be tested at their saturation (or near saturation) concentration and at a wide range. Each solution was tested with two replicates, except in the case of the  $\text{LiOH}$  0.2 M solution. In this case, due to experimental problems, the results of one specimen will be presented. The specimens were tested during one week under 40 V (electric field of 0.8 V/mm). This voltage was chosen as it is maximum voltage usually used in the field in treatments such as electrochemical chloride removal [25].

Passing current and catholyte temperature were continuously monitored and recorded by a data logger, while electrical resistance of the specimens and electrolyte pH were measured four times during the experiments. The electrical resistance was measured with a LCR-meter, in resistance mode at 120 Hz, while the specimens were still in the cells. During the experiment, the resistance was

**Table 2**  
Lithium solutions used as anolytes.

Salt	Concentration (M)	Salt	Concentration (M)
$\text{Li}_2\text{CO}_3$	0.2 (saturated)	$\text{LiNO}_3$	0.2
$\text{LiOH}$	0.2	$\text{LiNO}_3$	4.9
$\text{LiOH}$	4.9 (near saturation)	$\text{LiNO}_3$	7.8 (near saturation)

measured immediately after switching off the current. From the resistance, the specimen resistivity can be calculated with Eq. (1) [26], assuming that the resistance outside the specimens is zero:

$$\rho = \frac{RA}{L} \quad (1)$$

where  $R$  is the electrical resistance ( $\Omega$ ),  $A$  is the specimen surface area ( $\text{m}^2$ ) and  $L$  is the thickness of the specimen (m). Care should be taken when interpreting resistivity values, as they are strongly affected by temperature variations. Increase in temperature leads to drop in resistivity and vice versa. In fact, temperature may influence up to 5% with every K degree of variation [26]. The measurement on the eighth day was performed after 24 h without power, at room temperature.

The pH values of the electrolytes were obtained with a pH-meter, when it was possible. In the case of high pH (above 11) or high lithium concentration, pH test strips were used, in order to avoid pH-meter reading errors such as alkaline error [27]. Electrolyte samples were collected three times during the test and were analyzed by inductively coupled plasma optical emission spectroscopy (ICP-OES), in order to obtain the concentration of sodium, potassium, lithium and calcium (the last only in anolyte).

Ionic concentration profiles in mortar were obtained after the end of the test. To obtain these, the specimens were ground in a profile grinder in steps of 5.0 mm. The obtained powder (10–20 g) was then dissolved in boiling 3.0 M  $\text{HNO}_3$  (100 ml) and filtered to obtain a clear solution. The filtrate was washed with four parts of 10 ml of 1.0 M  $\text{HNO}_3$ . The obtained clear solution was then analyzed by ICP-OES for lithium, sodium and potassium.

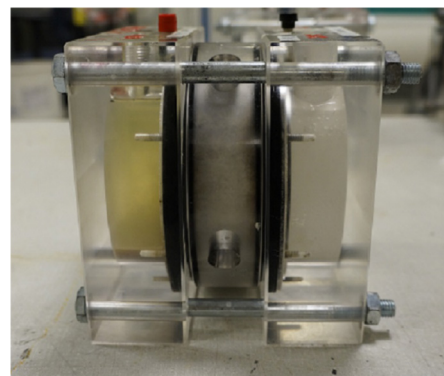
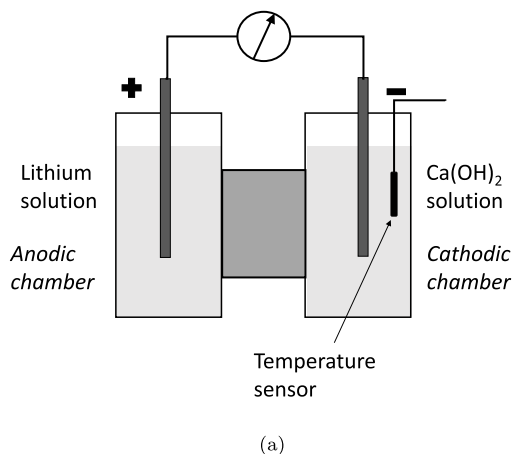
## 3. Results and discussion

Fig. 2(a) shows the current density that passed through all specimens during the migration experiment. The test with  $\text{LiNO}_3$  4.9 M (2) presented connection problems, as can be seen in the current density plot. The general behavior can be divided into three parts: in the first couple of hours, there was a rapid current increase, followed by a slower drop until around the third day. Finally, the

**Table 1**  
Cement composition, wt.% of cement.

CaO	$\text{SiO}_2$	$\text{Al}_2\text{O}_3$	$\text{Fe}_2\text{O}_3$	$\text{SO}_3$	MgO	$\text{P}_2\text{O}_5$	$\text{K}_2\text{O}$	$\text{TiO}_2$	$\text{Na}_2\text{O}$	Other	L.O.I. <sup>a</sup>
65.00	18.33	4.42	3.38	3.01	2.02	0.57	0.46	0.37	0.28	0.53	1.60

<sup>a</sup> L.O.I.: loss on ignition.



**Fig. 1.** Schematic diagram of the experimental set-up (a) and an experimental cell (b). Each electrolyte chamber contained 270 ml of solution.

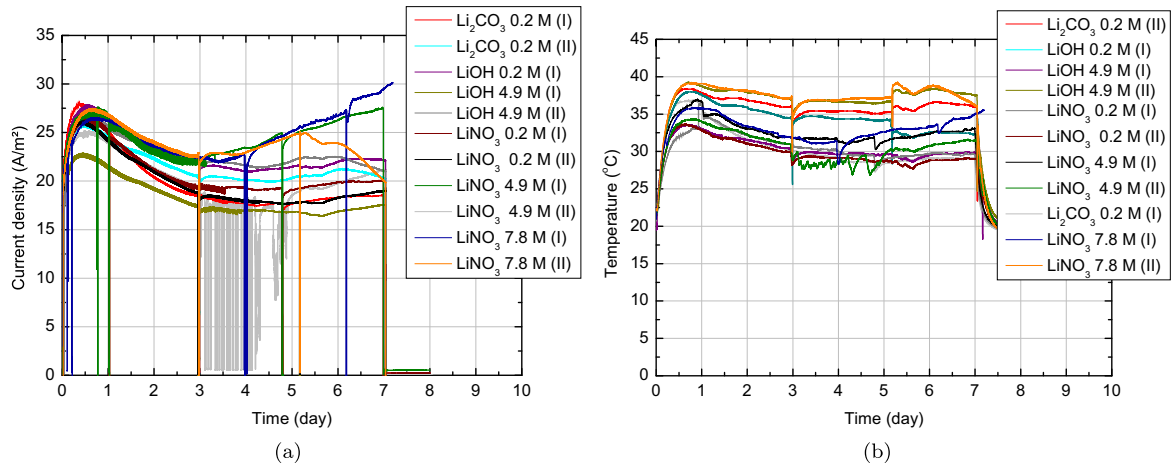


Fig. 2. Passing current density (a) and temperature (b) during the experiment.

Table 3

Passing charges during the experiments. The average between replicates and between specimens tested with solutions with the same concentration are presented.

Concentrations	0.2 M			4.9 M		7.8 M
Lithium compound	Li <sub>2</sub> CO <sub>3</sub>	LiOH	LiNO <sub>3</sub>	LiOH	LiNO <sub>3</sub>	LiNO <sub>3</sub>
Charge (kC)	95 (±4)	104	93 (±2)	93 (±10)	100 (±11)	112 (±3)
Av. charge (per conc.) (kC)		96 (±5)		97 (±11)		112 (±3)

current density stabilizes until the end of tests in the majority of the cells. This initial behavior was also noted by other authors [13,16] and it is believed to be due to the initially incomplete saturation of the specimens [13]. The overall trend is quite similar to what was reported by Liu et al. [16]. The temperature of the catholyte during the experiment can be seen in Fig. 2(b). In all cells, there was an increase in temperature, in particular, in the first few hours. This increase influenced the resistivity values, as will be further discussed.

The total charge that passed through the specimens can be calculated by the integration of their current plots, as shown in Eq. (2):

$$Q = \int_0^T i(t)dt \quad (2)$$

where  $Q$  is the charge that passed through the specimens (in C),  $i$  is the current (in A),  $T$  is the total time of the experiment (in s) and  $t$  is time (in s).

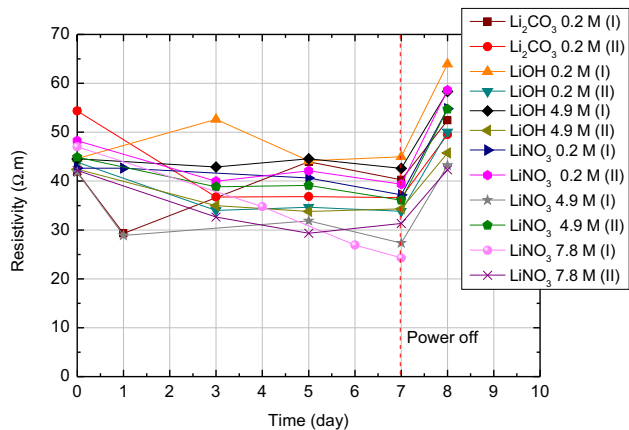


Fig. 3. Resistivity variations during the experiment.

Table 3 presents the total charges that passed through the cells. Overall, solutions with concentrations up to 4.9 M presented similar passing charges while the ones with 7.8 M had the highest charges.

In Fig. 3, specimen electrical resistivity variations during the experiment are shown. A summary is presented in Table 4. The resistivity of the specimen LiNO<sub>3</sub> 7.8 M (I) was not measured 24 h after the end of the experiment. For that reason, only the results for LiNO<sub>3</sub> 7.8 M (II) are presented in Table 4. The average initial resistivity was 45 ± 4 Ω.m. During the migration experiment, the increase in temperature noted in Fig. 2 led to a decrease in resistivity. Once the power was turned off and the cells cooled down to room temperature, the resistivity values were overall higher than the initial ones and the average was 51 ± 6 Ω.m. This

Table 4

Average (Av.) resistivity values at different moments of the experiment.

	Li <sub>2</sub> CO <sub>3</sub> 0.2 M	LiOH 0.2 M	LiNO <sub>3</sub> 0.2 M
	Av. (Ω.m)	Av. (Ω.m)	Av. (Ω.m)
Initial	48 ± 6	44	45 ± 3
Middle	40 ± 4	35	41 ± 1
End	38 ± 2	35	38 ± 1
After 24 h	51 ± 1	50	57 ± 2
	LiOH 4.9	LiNO <sub>3</sub> 4.9 M	
	Av. (Ω.m)	Av. (Ω.m)	
Initial	44 ± 1	43 ± 2	
Middle	39 ± 5	36 ± 4	
End	39 ± 4	32 ± 4	
After 24 h	52 ± 6	49 ± 6	
	LiNO <sub>3</sub> 7.8 M (II) <sup>a</sup>		
	Res. (Ω.m)		
Initial	42		
Middle	29		
End	31		
After 24 h	42		

<sup>a</sup> The resistivity of the specimen LiNO<sub>3</sub> 7.8 M (I) was not measured after 24 h. Thus, the average was not calculated and only the results for LiNO<sub>3</sub> 7.8 M (II) are presented in the table.

indicates that non-reversible modifications in pore structure and/or pore solution composition may have taken place. Liu et al. [16] observed the same behavior in their migration experiments. In fact, studies [28–31] have observed modifications in porosity due to the application of current. While Castellote et al. [28] found increasing total porosity in the regions near the anode and cathode due to the electric field application, other authors [29–31] have

pointed out that the application of current on concrete may lead to lower porosity and higher resistivity. Authors have suggested this could be due to the deposition of material in the pores [29,30].

Variations in pH in catholyte and anolyte are related to the cathodic and anodic reactions, respectively, as shown in the equations below. The cathodic reaction is shown in Eq. (3) and produces hydroxyl ions, leading to an increase of pH. The reaction that takes

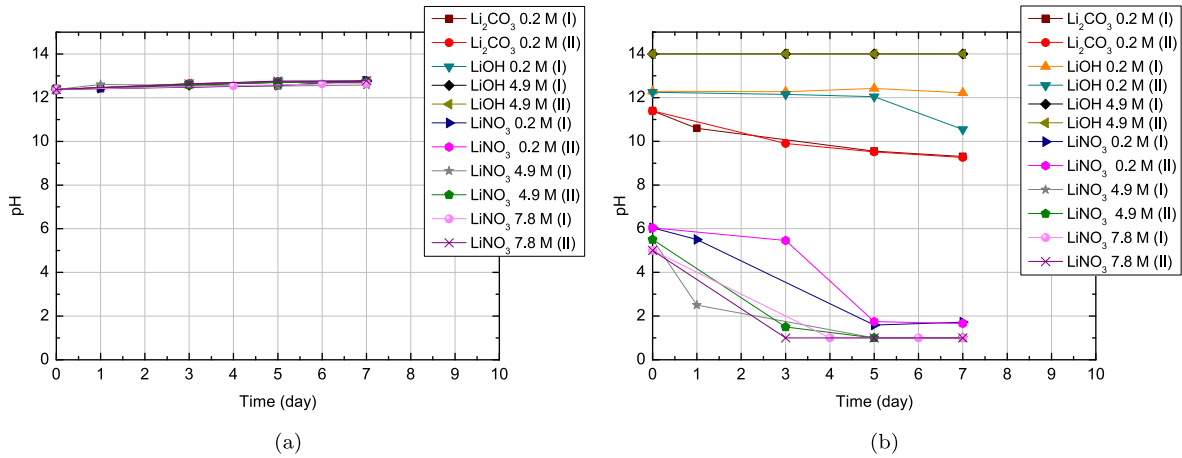


Fig. 4. pH variations in catholyte (a) and anolyte (b) during the experiments.

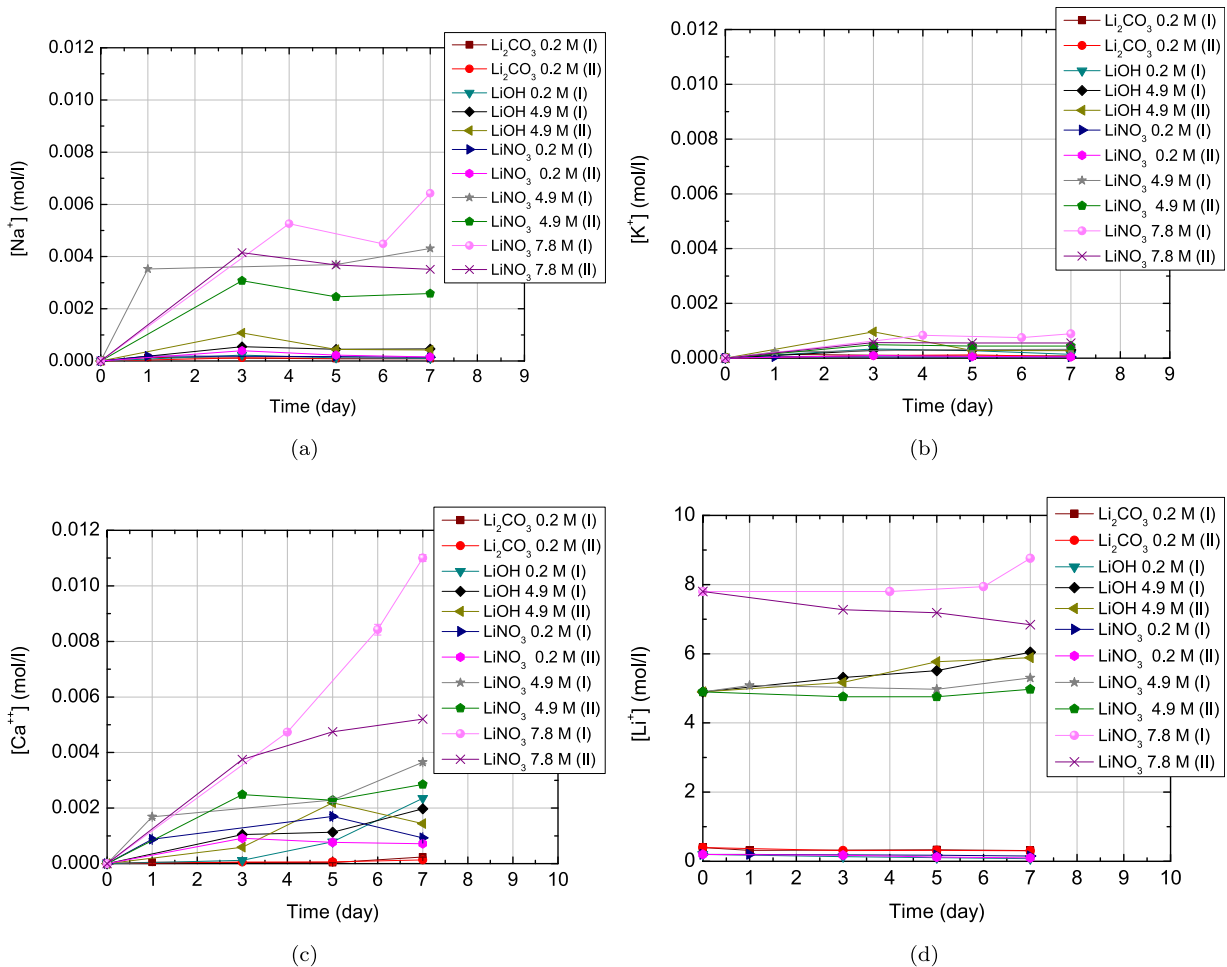


Fig. 5. Variations in concentration in anolyte solutions of sodium (a), potassium (b), calcium (c) and lithium (d).

place at the anode depends on the pH of the solution: if it is basic, Eq. (4) occurs. Otherwise, Eq. (5) happens. Either way, the anodic reactions decrease the pH of the solution.



Fig. 4 presents the pH variations in catholyte (a) and anolyte (b) solutions during the experiment. Initially, the catholyte solutions exhibited a pH around 12 and, throughout the test, their pH increased very slightly. The progress of the anolyte pH, on the other hand, as shown in Eqs. (4) and (5), depended on the initial value. The passing charge also influenced the pH: the higher the passing charge in LiNO<sub>3</sub> solutions, for example, the more rapid and stronger was the acidification of the solution. All LiNO<sub>3</sub> solutions were initially nearly neutral and they presented the highest pH drops during the test. In fact, the anodes of those cells presented corrosion, due to the low pH and strong anodic polarization. Both LiOH - 4.9 M solutions had very basic initial pH (14) and it remained at that level until the end of the experiment. It is interesting to notice that, although Li<sub>2</sub>CO<sub>3</sub> and LiOH 0.2 M solutions had close initial pH, LiOH solution had better buffer capacity and the pH showed a slower decrease.

Chemical compositions of anolyte solutions can be seen in Fig. 5. Sodium, potassium and calcium ions move from the speci-

men to the anolyte due to diffusion and dissolution of the hydrated phases. The latter happened especially in the cells with LiNO<sub>3</sub> 4.9 and 7.8 M solutions, due to the acidification of the anolyte. Acids, with pH below 4.5, severely attack concretes (or mortars), by dissolving Ca(OH)<sub>2</sub> and removing calcium ions from hydrated silicates and aluminates [32,33]. This explains why the LiNO<sub>3</sub> anolytes presented higher concentrations of those three ions - especially calcium. Lithium concentration in the anolyte was supposed to decrease, as lithium ions are transported into the specimen. Nevertheless, in some tests, that was not the case. This is probably because of changes in the volume of water by evaporation, only visually observed and estimated to be around 10–20%. This means that the concentrations presented for the other ions are likely to be overestimated.

As expected, sodium and potassium concentrations in the catholytes increased with time, as those ions left the pore solution of the specimens, as shown in Fig. 6. Potassium ions left the specimen faster, especially in the first days, because of its higher ionic mobility and higher concentration in the pore solution. Fig. 6 shows the detectable amounts of lithium concentration in the catholyte. For most cells, it took at least 5 days for lithium ions to reach the cathodic chamber. The cells with LiNO<sub>3</sub> 4.9 and 7.8 M presented the highest levels of lithium in the catholyte.

Fig. 7 exhibits total sodium and potassium concentration profiles in the specimens after the experiment. The initial content was obtained from a specimen that did not go through the migration test. As the concentrations were obtained from ground samples, ions from the pore solution or bound and/or adsorbed to the solid phases are not distinguished. As expected, all specimens

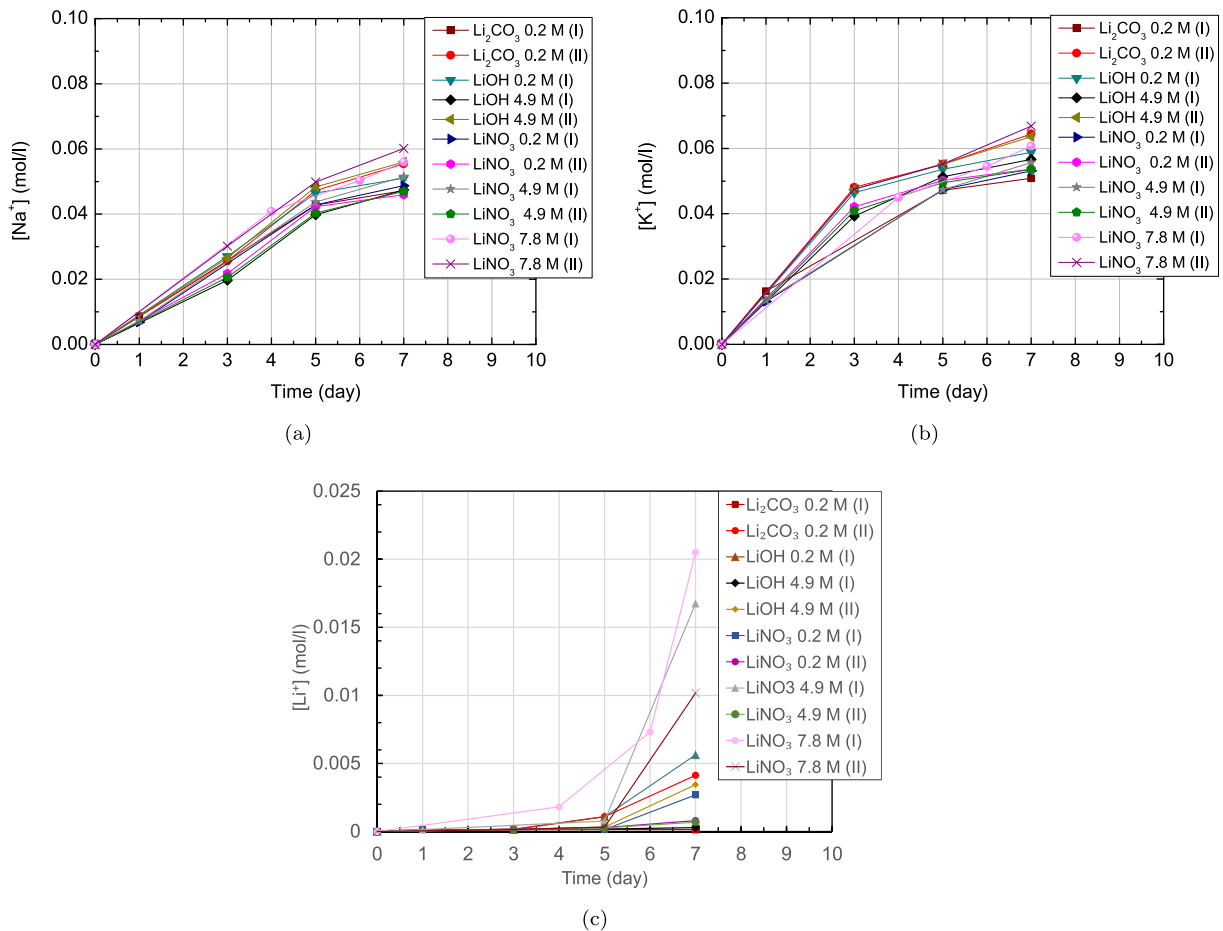


Fig. 6. Variations in concentration in catholyte solutions of sodium (a), potassium (b) and lithium (c).



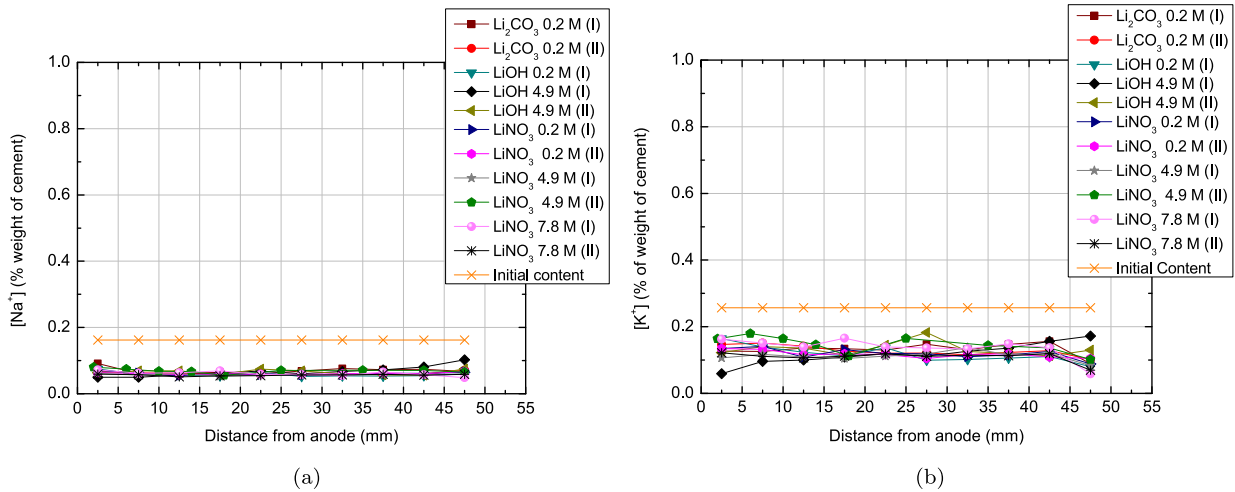


Fig. 7. Sodium (a) and potassium (b) concentration profile in the specimen after test.

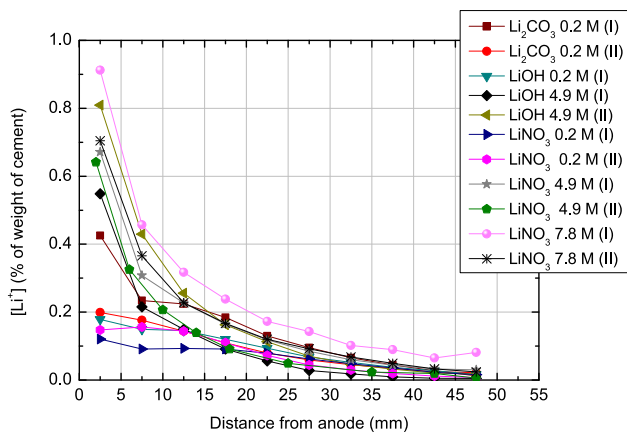


Fig. 8. Lithium concentration profile in the specimens after test.

showed lower concentrations of sodium and potassium than the initial content. Furthermore, the profiles were more or less constant for most specimens. This may indicate that all (or most of) free sodium and potassium ions had left the specimen by the end of the test and the ones that were measured were actually bound and/or adsorbed to solid phases. In fact, Liu et al. [16] obtained the same type of constant profile, after longer experiments. In addition, they also monitored the sodium and potassium concentrations in the catholyte and noted that, after some time, they became constant until the end of the experiment. The authors then concluded that all free sodium and potassium had left the specimens.

Lithium concentration profiles in the specimen are shown in Fig. 8. All profiles exhibit similar basic shape, in which the concentration is higher close to the anode and it decreases towards the cathode. A sharp concentration front would be expected for a migration experiment through a porous medium [13]. However,

this was not the case. In fact, other authors have found the same type of profile in their works (e.g. [13,16,14]).

In the first 10 mm from the anode, all specimens that were treated with lithium solutions with 4.9 M and 7.8 M presented higher lithium content. However, in deeper layers, the cases LiOH 4.9 M (I) and LiNO<sub>3</sub> 4.9 M (II) exhibited lower levels. In fact, LiOH 4.9 M (I), in the last 25 mm, presented the lowest lithium concentrations. This is probably related to the elevated sodium and potassium levels in the same specimen in that region (Fig. 7). It is worth noting that the final resistivity values of these specimens are among the highest in Fig. 3. The increase in resistivity may explain their lithium profiles. Interestingly, beyond the first 10 mm, the specimen Li<sub>2</sub>CO<sub>3</sub> 0.2 M (I) presented higher lithium content than the other cases with lithium solution at 0.2 M, probably due to its lower initial resistivity (Fig. 3). Interestingly, even though the Li<sub>2</sub>CO<sub>3</sub> 0.2 M (II) presented similar final lithium levels as the other specimens treated with 0.2 M solutions. The average amounts of lithium in the specimens can be seen in Table 5. Although some variations between replicates are fairly high, the overall trend indicates that the specimens with highest lithium contents had been treated with lithium solutions with concentrations of 4.9 or 7.8 M. This is confirmed by the plot of Fig. 9 which shows the total amount of lithium ions in the specimens after migrations for the different initial concentrations of lithium ions.

Fig. 10 shows the lithium to sodium plus potassium molar ratio ( $\frac{[Li]}{[Na+K]}$ ) in the specimens after test. When lithium is used as admixture, it is known that the ratio to prevent deleterious ASR expansion depends on the type of lithium compound and aggregate. It is generally accepted that the minimum ratio varies from 0.65 to 1.00 [6]. If the upper limit is considered, only the specimen LiNO<sub>3</sub> 7.8 M (I) is fully treated, with  $\frac{[Li]}{[Na+K]}$  above 1.0 in all regions. Most specimens would be treated until 35 mm from the anode, while LiOH 4.9 M (I) and LiNO<sub>3</sub> 4.9 M (II), only until 25 mm. Nevertheless, results should be interpreted with care - the mechanism to stop ASR expansion is not necessarily the same that takes place when

Table 5  
Average concentration of lithium in the specimens after experiments.

Concentrations	0.2 M		4.9 M		7.8 M	
Lithium compound	Li <sub>2</sub> CO <sub>3</sub>	LiOH	LiNO <sub>3</sub>	LiOH	LiNO <sub>3</sub>	LiNO <sub>3</sub>
Average Li (wt.% of cement)	0.12 ± 0.03	0.09	0.07 ± 0.01	0.15 ± 0.04	0.17 ± 0.01	0.22 ± 0.04
Av. per conc. (wt.% of cement)		0.09 ± 0.03		0.16 ± 0.03		0.22 ± 0.04



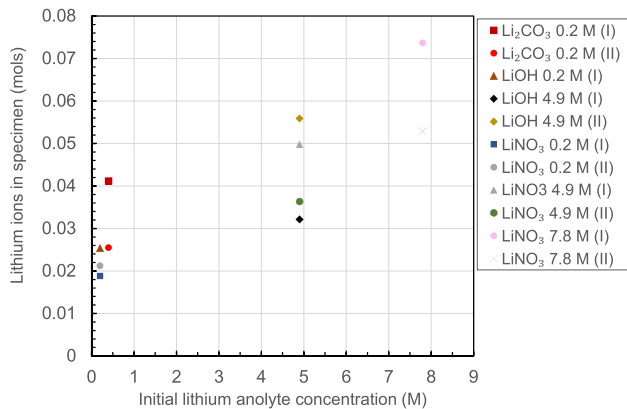


Fig. 9. Total amount of lithium ions in the specimen after test per initial lithium concentration in anolyte solutions.

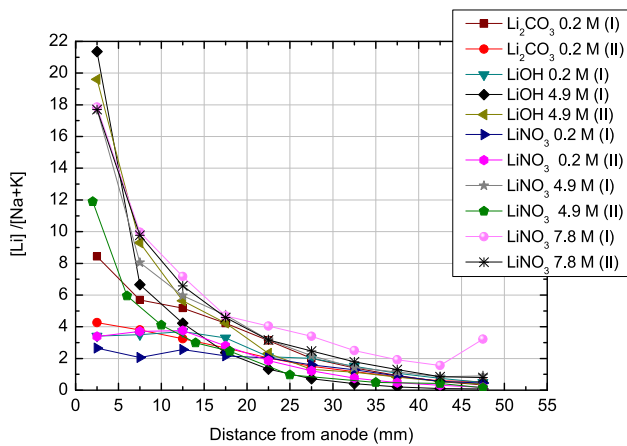


Fig. 10. Lithium to alkalis molar ratio in the specimen after test.

lithium admixtures are used. It is possible that, in the case of treatment, other  $\frac{[Li]}{[Na+K]}$  ratios should be reached in order to stop (or reduce) ASR expansion.

#### 4. Conclusions

In this paper, the influence of the type and concentration of the anolyte solution on lithium migration was investigated. The following conclusions can be drawn.

- The lithium concentration in the anolyte, rather than the type of lithium salt in it, plays a role on final lithium content in the specimen. The higher is the concentration the more lithium goes into the mortar.  $\text{LiNO}_3$  7.8 M solutions were the ones that presented the highest levels of lithium after the experiment.
- Migration, under the tested conditions (for a week under 40 V), led to increase of resistivity of the specimens.
- The use of  $\text{LiNO}_3$  solutions led to the acidification of the anolyte solution. Although, under visual inspection, the specimens did not show deterioration, the chemical compositions of the anolyte indicate that acid attack took place in those cases. In addition, the low pH and the high anodic polarization caused corrosion of the anodes.
- Most, if not all, free sodium and potassium left the specimen during the one week experiments and it took around five days for lithium to go through the specimens and arrive in the catholyte solutions of most cells.

#### 5. Conflict of interest

The authors declared that there is no conflict of interest.

#### Acknowledgment

Funding: This work was supported by Dutch Technology Foundation STW, Sika Technology AG, BAM Infraconsult BV, Rijkswaterstaat, TNO Delft, Van Nieuwpoort Grint en Zand B.V., TCKI - Stichting Technisch Centrum voor de Keramische Industrie and Care4Concrete (STW project 10971: "Modelling, non-destructive testing and Li-based remediation of deleterious Alkali-Silica Reaction in concrete structures").

#### References

- [1] F. Rajabipour, E. Giannini, C. Dunant, J.H. Ideker, M.D. Thomas, Alkali-silica reaction: current understanding of the reaction mechanisms and the knowledge gaps, *Cem. Concr. Res.* 76 (2015) 130–146, <https://doi.org/10.1016/j.cemconres.2015.05.024>.
- [2] P.J. Nixon, I. Sims, RILEM Recommendations for the Prevention of Damage by Alkali-Aggregate Reactions in New Concrete Structures: State-of-the-Art Report of the RILEM Technical Committee 219-ACS, vol. 17, Springer, 2015, <https://doi.org/10.1007/978-94-017-7252-5>.
- [3] W. McCoy, A. Caldwell, New approach to inhibiting alkali-aggregate expansion, *ACI Journal Proceedings*, vol. 47, ACI, 1951.
- [4] D. Stark, B. Morgan, P. Okamoto, Eliminating or minimizing alkali-silica reactivity, *Tech. Rep. SHRP-C-343*, Strategic Highway Research Program, 1993.
- [5] K. Ramyar, O. Çopuroğlu, Ö. Andıç, A. Fraaij, Comparison of alkali-silica reaction products of fly-ash-or lithium-salt-bearing mortar under long-term accelerated curing, *Cem. Concr. Res.* 34 (7) (2004) 1179–1183, <https://doi.org/10.1016/j.cemconres.2003.12.007>.
- [6] X. Feng, M. Thomas, T. Bremner, B. Balcom, K. Folliard, Studies on lithium salts to mitigate ASR-induced expansion in new concrete: a critical review, *Cem. Concr. Res.* 35 (9) (2005) 1789–1796, <https://doi.org/10.1016/j.cemconres.2004.10.013>.
- [7] X. Feng, M. Thomas, T. Bremner, K.J. Folliard, B. Fournier, New observations on the mechanism of lithium nitrate against alkali silica reaction (asr), *Cem. Concr. Res.* 40 (1) (2010) 94–101, <https://doi.org/10.1016/j.cemconres.2009.07.017>.
- [8] K.J. Folliard, M.D. Thomas, B. Fournier, K.E. Kurtis, J.H. Ideker, Interim recommendations for the use of lithium to mitigate or prevent alkali-silica reaction (ASR), *Tech. Rep. FHWA-HRT-06-073*, Federal Highway Administration, 2006.
- [9] M. Thomas, D. Stokes, Lithium impregnation of ASR-affected concrete: preliminary studies, in: *Proceedings of the 12th International Conference on Alkali-Aggregate Reaction in Concrete*, 2004, pp. 659–667.
- [10] A. Santos Silva, M. Salta, M. Melo Jorge, M. Rodrigues, A. Cristiano, Research on the suppression expansion due to ASR. Effect of coatings and lithium nitrate, in: *Proceedings of the 13th International Conference on Alkali-Aggregate Reaction in Concrete*, 2008.
- [11] C. Page, Interfacial effects of electrochemical protection methods applied to steel in chloride-containing concrete, in: *Proceedings of International Conference on Rehabilitation of Concrete Structures*, 1992, pp. 179–187.
- [12] D. Whitmore, S. Abbott, Use of an applied electric field to drive lithium ions into alkali-silica reactive structures, in: *Proceedings, 11th International Conference on Alkali-Aggregate Reaction*, 2000, pp. 1089–1098.
- [13] J. Pacheco, R.B. Polder, Preliminary study of electrochemical lithium migration into cementitious mortar, in: *2nd International Symposium on Service Life Design for Infrastructures*, RILEM Publications SARL, 2010, pp. 1093–1100.
- [14] T. Ueda, Y. Baba, A. Nanasawa, Penetration of lithium into ASR affected concrete due to electro-osmosis of lithium carbonate solution, *Constr. Build. Mater.* 39 (2013) 113–118, <https://doi.org/10.1016/j.conbuildmat.2012.05.007>.
- [15] T. Ueda, J. Kushida, M. Tsukagoshi, A. Nanasawa, Influence of temperature on electrochemical remedial measures and complex deterioration due to chloride attack and ASR, *Constr. Build. Mater.* 67 (2014) 81–87, <https://doi.org/10.1016/j.conbuildmat.2013.10.020>.
- [16] C.-C. Liu, W.-C. Wang, C. Lee, Behavior of cations in mortar under accelerated lithium migration technique controlled by a constant voltage, *J. Mar. Sci. Technol.* 19 (1) (2011) 26–34.
- [17] L.M.S. Souza, R.B. Polder, O. Çopuroğlu, Lithium migration in mortar specimens with embedded cathode, in: *Concrete Repair, Rehabilitation and Retrofitting IV: Proceedings of the 4th International Conference on Concrete Repair, Rehabilitation and Retrofitting (ICRRR-4)*, 5–7 October 2015, Leipzig, Germany, CRC Press, 2015, p. 39, <https://doi.org/10.1201/b18972-8>.
- [18] L.M.S. Souza, Electrochemical lithium migration to mitigate alkali-silica reaction in existing concrete structures (Ph.D. thesis), Delft University of Technology, 2016. URL: <https://doi.org/10.4233/uuid:443835f4-d172-4267-8412-dd3cfe24330a>.

- [19] L.M.S. Souza, R.B. Polder, O. Çopuroğlu, Lithium migration in a two-chamber set-up as treatment against expansion due to alkali-silica reaction, *Constr. Build. Mater.* 134 (2017) 324–335, <https://doi.org/10.1016/j.conbuildmat.2016.12.052>.
- [20] T. Ueda, A. Nanasawa, M. Tsukagoshi, Influence of electrochemical lithium penetration from various kinds of lithium solution on ASR expansion of concrete, in: *Proceedings of the 4th International Conference on Concrete Repair, Rehabilitation and Retrofitting*, CRC Press, 2015.
- [21] N.-E. 196-1, *Methods of testing cement - part 1: Determination of strength*, 2005.
- [22] N.-E. 12350-7, *Testing fresh concrete - part 7: Air content - pressure methods*, 2009.
- [23] N.-E. 12350-5, *Testing fresh concrete - part 5: Air content - flow table test*, 2009.
- [24] ASTM-C1202-05, *Standard test method for electrical indication of concrete's ability to resist chloride ion penetration*, 2005. <https://doi.org/10.1520/C1202-12>.
- [25] L. Bertolini, B. Elsener, P. Pedferri, E. Redaelli, R.B. Polder, *Corrosion of Steel in Concrete: Prevention, Diagnosis, Repair*, second ed., John Wiley & Sons, 2013, <https://doi.org/10.1002/9783527651696>.
- [26] R.B. Polder, Test methods for on site measurement of resistivity of concrete - a RILEM TC -154 technical recommendation, *Construction Building Mater.* 15 (2) (2001) 125–131, [https://doi.org/10.1016/S0950-0618\(00\)00061-1](https://doi.org/10.1016/S0950-0618(00)00061-1).
- [27] W. Boyes, *Instrumentation Reference Book*, Butterworth-Heinemann, 2009.
- [28] M. Castellote, C. Andrade, M.C. Alonso, Changes in concrete pore size distribution due to electrochemical chloride migration trials, *Mater. J.* 96 (3) (1999) 314–319.
- [29] P. Banfill, Re-alkalisation of carbonated concrete - effect on concrete properties, *Constr. Build. Mater.* 11 (4) (1997) 255–258, [https://doi.org/10.1016/S0950-0618\(97\)00045-7](https://doi.org/10.1016/S0950-0618(97)00045-7).
- [30] M. Siegwart, J.F. Lyness, B.J. McFarland, Change of pore size in concrete due to electrochemical chloride extraction and possible implications for the migration of ions, *Cem. Concr. Res.* 33 (8) (2003) 1211–1221, [https://doi.org/10.1016/S0008-8846\(03\)00047-4](https://doi.org/10.1016/S0008-8846(03)00047-4).
- [31] D. Koleva, O. Copuroglu, K. van Breugel, G. Ye, J. De Wit, Electrical resistivity and microstructural properties of concrete materials in conditions of current flow, *Cement and Concrete Composites* 30 (8) (2008) 731–744, <https://doi.org/10.1016/j.cemconcomp.2008.04.001>.
- [32] H.F. Taylor, *Cement Chemistry*, Thomas Telford, 1997.
- [33] A.M. Neville, *Properties of concrete*, fifth ed., Pearson, 2011.